

Preparation, radiolabeling and cell culture studies of chitosan coated PLGA nanoparticles as a potential cancer diagnostic agent

Meliha EKİNCİ¹ , A. Alper ÖZTÜRK² , Derya İLEM-ÖZDEMİR^{1*} 

¹ Department of Radiopharmacy, Faculty of Pharmacy, Ege University, Bornova 35040 Izmir, Türkiye.

² Department of Pharmaceutical Technology, Faculty of Pharmacy, Anadolu University, Tepebaşı 26210 Eskisehir, Türkiye.

* Corresponding Author. E-mail: deryailem@gmail.com (D.İ.Ö.); Tel. +90-232-311 19 63.

Received: 25 April 2022 / Revised: 22 June 2022 / Accepted: 29 June 2022

ABSTRACT: Using the nanoprecipitation process, chitosan coated poly lactic-co-glycolic acid (PLGA) based polymeric nanoparticle formulations of two molecular weights were developed as a possible cancer cell diagnostic agent. Photon correlation spectroscopy was used to measure the particle size, distribution [polydispersity index (PDI)], and zeta potential values of developed nanoparticle formulations. The F1 [low molecular weight PLGA (Resomer® RG 503 H)] and F2 [high molecular weight PLGA (Resomer® RG 504 H)] formulations were then directly labeled with Technetium-99m ($[^{99m}\text{Tc}]\text{Tc}$) using stannous salts (chloride) as a reducing agent. The radiochemical purity (RP) and *in vitro* stability in different mediums of the formulations were assessed using ascending radioactive thin layer chromatography (RTLC) method. The cell incorporation of $[^{99m}\text{Tc}]\text{Tc}$ labeled F1 and F2 formulations, as well as Reduced/Hydrolyzed $[^{99m}\text{Tc}]\text{NaTcO}_4$ (R/H- $[^{99m}\text{Tc}]\text{NaTcO}_4$) in the MCF-7 (breast cancer cell line) cells, was then assessed. The nanoparticles had a middle size of 408.9 ± 3.626 nm to 421.3 ± 7.205 nm, a PDI value of 0.310 ± 0.055 to 0.330 ± 0.066 , and a positive charge of $+70.5 \pm 1.4$ mV to $+75.5 \pm 3.8$ mV, according to the characterization results. F1 and F2 formulations were effectively radiolabeled with $[^{99m}\text{Tc}]\text{Tc}$, and their RP was found to be over 98% in both cases. When compared to $[^{99m}\text{Tc}]\text{Tc}$ -F1 ($45.091 \pm 2.254\%$) and R/H- $[^{99m}\text{Tc}]\text{NaTcO}_4$ ($8.527 \pm 0.426\%$), the incorporation percentages of $[^{99m}\text{Tc}]\text{Tc}$ -F2 ($70.756 \pm 3.537\%$) were shown to be higher in cancer cell lines (breast cancer cells, MCF-7). According to this research, radiolabeled chitosan coated PLGA nanoparticles ($[^{99m}\text{Tc}]\text{Tc}$ -F2) could be suggested as promising cancer detection formulations. However, further investigations, such as biodistribution studies, should be performed.

KEYWORDS: Chitosan; PLGA; nanoparticle; diagnostic nanosystem; technetium-99m; radiolabeling; cell culture.

1. INTRODUCTION

Cancer has long been one of the leading causes of death worldwide [1]. Breast cancer is one of the most common malignancies faced by women around the world [2]. Treatment of breast cancer can be quite effective, with survival rates of 90 percent or more, especially when the disease is detected early. Major problems in the treatment of breast cancer include treatment resistance, recurrence, and metastasis [3]. Early diagnosis and effective treatment of breast cancer therefore significantly reduces treatment costs, treatment duration, and the risk of mortality and morbidity [4].

Various nanocomposites have been developed for cancer treatment and diagnosis, including nanoparticles, liposomes, micelles, niosomes, drug-loaded particles, dendrimers, etc. [5,6]. Controlled drug delivery, gene therapy, radiolabeled diagnosis and therapy, cancer immunotherapy, receptor-specific and anticancer drug delivery are just some of the biocompatible polymeric drug delivery systems developed in the last century [7-10]. Due to its biocompatibility and biodegradability, polymilk-co-glycolic acid (PLGA) is one of the most commonly used polymers for drug delivery systems [11-13]. Chitosan is a natural biopolymer produced from deacetylated chitin. It has been carefully explored in an interdisciplinary approach for a variety of applications. Chitosan-based biomaterials have antifungal and antibacterial properties as well as mucoadhesion, nontoxicity, biodegradability, and biocompatibility. In addition, chitosan is a naturally occurring polysaccharide that can be chemically modified for a variety of uses and functions [14]. Due to the free protonatable amino groups in the chitosan backbone and the flexibility of the

How to cite this article: Ekinci M, ÖzTÜRK AA, İLEM-ÖZDEMİR D. Preparation, radiolabeling and cell culture studies of chitosan coated PLGA nanoparticles as a potential cancer diagnostic agent. J Res Pharm. 2022; 26(6): 1636-1645.

chitosan structure, it is easy to modify and functionalize chitosan into a nanoparticle system with high adaptability in cancer treatment [15]. The use of chitosan-coated PLGA nanoparticles as a drug delivery technology remains important due to the excellent biocompatibility of the system [15-17].

Radionuclides are employed as signal sources in the development of drugs because they can be incorporated into formulations without changing their physical and biological properties. The primary benefit of using radiolabeled formulations in drug development is that they are highly sensitive and detectable in little amounts [18,19]. The radionuclide to be used in the construction of powerful radiotracers must be carefully chosen. Technetium-99m ($[^{99m}\text{Tc}]\text{Tc}$) is one of the most used radionuclide for radiolabeling of drug delivery systems because of its adaptable chemistry, 140 KeV of pure gamma energy, minimal radiation dose, and 6 h of short half-life [19].

The purpose of this research is to compare the applicability of chitosan-coated PLGA nanoparticles containing PLGA of two molecular weights as a cancer diagnostic agent in a cancer cell line (model cancer cell line: breast cancer cells, MCF-7). To do this, using the nanoprecipitation method, two different nanoparticle formulations (F1 and F2 formulations) were developed. Then, nanoparticles were radiolabeled with $[^{99m}\text{Tc}]\text{Tc}$ using the stannous chloride method, and radiolabeled nanoparticles were subjected to quality control using radioactive thin layer chromatography (RTLC). The stability of radiolabeled formulations in different mediums and partition coefficient studies were investigated. Finally, in MCF-7 cell lines, a comparative *in vitro* cell culture investigation of radiolabeled nanoparticles and R/H- $[^{99m}\text{Tc}]\text{NaTcO}_4$ was performed.

2. RESULTS AND DISCUSSION

2.1. Preparation and characterization of chitosan coated PLGA nanoparticles

Chitosan coated PLGA-based nanoparticles were successfully produced and lyophilized using the nanoprecipitation process [13,20-22]. Table 1 shows DLS data for F1 and F2. Nanoparticles must meet two crucial criteria: particle size and PDI. Release rate of the drug, biodistribution, mucoadhesion, cellular uptake of water and buffer transfer to the core of nanoparticles, protein diffusion, and treatment are all influenced by these features [23]. To measure the size of Brownian particles in colloidal dispersion at nano and micron intervals, the quickest and most popular techniques, such as DLS or photon-correlation spectroscopy (PCS), are extensively used [24,25]. In this study, DLS is used since it is the most widely used approach for estimating particle size and PDI. F1 and F2 had an average diameter of between 408.9 ± 3.626 nm and 421.3 ± 7.205 nm and the PDI of between 0.310 ± 0.055 and 0.330 ± 0.066 . According to the particle size results, literature supports the production of nano-sized nanoparticles under submicron [26]. The PDI value that describes size distribution for monophasic systems is in the range of 0.01 to 0.5; values higher than 0.5 imply a very wide size distribution, while values approaching zero indicate a narrow size distribution [27]. All of the PDI values were less than 0.5. Quality and monodisperse chitosan coated PLGA nanoparticles have been synthesized, according to the literature.

Table 1. The DLS results of nanoparticles

Formulations	Particle size (nm \pm SD)	PDI (\pm SD)	Zeta potential (mV \pm SD)
F1	421.3 ± 7.205	0.310 ± 0.055	$+75.5 \pm 3.8$
F2	408.9 ± 3.626	0.330 ± 0.066	$+70.5 \pm 1.4$

The positive zeta potential value of F1 and F2 was between $+70.5 \pm 1.4$ mV and $+75.5 \pm 3.8$ mV. The chemical structure of chitin and chitosan is the same. Chitin is an acetylglucosamine linear chain. Chitosan is made by removing enough acetyl groups ($\text{CH}_3\text{-CO}$) from a molecule so that it may be dissolved in most diluted acid solutions. Deacetylation is a chemical process that produces cationic chitosan by releasing amine groups (-NH). Another theory is that chitosan is made by alkaline deacetylation of chitin, one of nature's most frequent polymers, resulting in a polymer made up of two subunits, N-acetyl-d-glucosamine and d-glucosamine, connected by 1,4-glycosidic linkages. Because chitosan's glucosamine core has a protonable high density -NH, nanoparticles produced or coated with it have a positive zeta potential [27]. The presence of chitosan is the explanation for the positive zeta potential value. Due to the translocation of negatively charged components of the inner layer of the cell membrane (such as anionic phospholipids, phosphatidylserine, proteoglycans, and glycoproteins) to the cell surface, cell surfaces, particularly cancer cell surfaces, are typically negatively charged. PLGA in neutral media has negative surface potential, because of terminal carboxyl groups. Targeting and interacting with cells can frequently be challenging for

PLGA nanoparticles. For this reason, we performed surface modification with chitosan to enable the nanoparticles to interact with negatively charged cancer cells and to convert the negative zeta potential of PLGA to positive [12].

2.2. Radiolabeling and RTLC studies

A simple, quick, and effective directly labeling approach was used to label nanoparticles with [^{99m}Tc]Tc. For quality control studies, RTLC tests were used to evaluate the labeling efficiency of the [^{99m}Tc]Tc-F1 and [^{99m}Tc]Tc-F2. To differentiate and measure the levels of radioactive contaminant (Free [^{99m}Tc]NaTcO₄ and Reduced/Hydrolized (R/H)-[^{99m}Tc]NaTcO₄), acetone and pyridine/acetic acid/water (3:5:1.5) were utilized. Free [^{99m}Tc]NaTcO₄ migrated with the solvent front in RTLC using acetone as the mobile phase (*Rf* = 0.8-1.0), while [^{99m}Tc]Tc-F1 and [^{99m}Tc]Tc-F2 remained at the spotting point (*Rf* = 0.0-0.2). Also, [^{99m}Tc]Tc-F1, [^{99m}Tc]Tc-F2 and free [^{99m}Tc]NaTcO₄ migrated with the solvent front in RTLC using pyridine/acetic acid/water (3:5:1.5) as the mobile phase (*Rf* = 0.8-1.0), R/H-[^{99m}Tc]NaTcO₄ remained at the spotting point (*Rf* = 0.0-0.2). The RP of [^{99m}Tc]Tc-F1 and [^{99m}Tc]Tc-F2 formulations including different amount of reducing agent were shown in Table 2 and Table 3.

Table 2. Radiolabeling efficiency of [^{99m}Tc]Tc-F1 formulation including different amount of reducing agent

[^{99m} Tc]Tc-F1 (%)	Stannous chloride amount ($\mu\text{g.mL}^{-1}$)			
Time (h)	10 $\mu\text{g.mL}^{-1}$	25 $\mu\text{g.mL}^{-1}$	50 $\mu\text{g.mL}^{-1}$	100 $\mu\text{g.mL}^{-1}$
0.25	89.34 ± 0.59	92.26 ± 1.15	95.78 ± 0.46	99.42 ± 0.16
1	90.12 ± 1.10	93.47 ± 0.99	95.68 ± 1.73	99.52 ± 0.08
2	89.63 ± 1.03	91.68 ± 0.17	94.93 ± 1.79	98.51 ± 0.17
3	89.36 ± 0.87	92.76 ± 1.61	96.30 ± 0.78	98.69 ± 0.15
4	90.03 ± 0.65	92.78 ± 0.69	95.07 ± 1.63	99.68 ± 0.10
5	89.14 ± 0.46	93.05 ± 1.11	94.76 ± 0.75	98.53 ± 0.07
6	88.10 ± 0.78	91.63 ± 0.77	95.36 ± 1.49	98.44 ± 0.04

Table 3. Radiolabeling efficiency of [^{99m}Tc]Tc-F2 formulation including different amount of reducing agent

[^{99m} Tc]Tc-F2 (%)	Stannous chloride amount ($\mu\text{g.mL}^{-1}$)			
Time (h)	10 $\mu\text{g.mL}^{-1}$	25 $\mu\text{g.mL}^{-1}$	50 $\mu\text{g.mL}^{-1}$	100 $\mu\text{g.mL}^{-1}$
0.25	90.39 ± 0.46	93.46 ± 0.36	96.53 ± 0.98	99.43 ± 0.12
1	88.63 ± 0.67	94.63 ± 1.04	97.83 ± 1.10	99.50 ± 0.06
2	89.11 ± 1.64	93.47 ± 0.74	96.46 ± 0.68	98.61 ± 0.11
3	87.57 ± 0.49	92.36 ± 0.44	96.36 ± 0.75	98.63 ± 0.17
4	89.42 ± 0.64	92.85 ± 1.10	96.75 ± 1.16	99.32 ± 0.07
5	89.61 ± 0.06	91.36 ± 0.58	95.38 ± 0.47	99.40 ± 0.18
6	88.47 ± 0.39	91.74 ± 1.07	95.43 ± 1.12	98.65 ± 0.03

[^{99m}Tc]NaTcO₄ has +7 valence when eluted from the Molybdenum-99 ([^{99m}Mo]Mo)/[^{99m}Tc]Tc generator and cannot bond with any compound or formulation. In order for [^{99m}Tc]NaTcO₄ to bond, the valency of +7 must be lowered (+4/+5) with the use of reducing agents. For this purpose, reducing agents such as stannous chloride, stannous tartrate or sodium borohydride are often used in radiolabeling studies with [^{99m}Tc]NaTcO₄ [28]. Herein, stannous chloride was utilized for direct radiolabeling of F1 and F2 with [^{99m}Tc]NaTcO₄, and the role of the reducing agent on the radiolabeling process was investigated using varied stannous chloride amounts (10, 25, 50 and 100 $\mu\text{g.mL}^{-1}$). The optimum reducing agent amount was determined to be 100 $\mu\text{g.mL}^{-1}$ based on labeling efficiency. Both nanoparticle formulations were radiolabeled by [^{99m}Tc]NaTcO₄ with high RP ($\geq 98\%$) in the presence of 100 $\mu\text{g.mL}^{-1}$ reducing agent. The complex was found to be highly stable for up to 6 h without affecting the labeling yield significantly ($p > 0.05$). The RTLC chromatogram of [^{99m}Tc]Tc-F1 and [^{99m}Tc]Tc-F2 were shown in Figure 1.

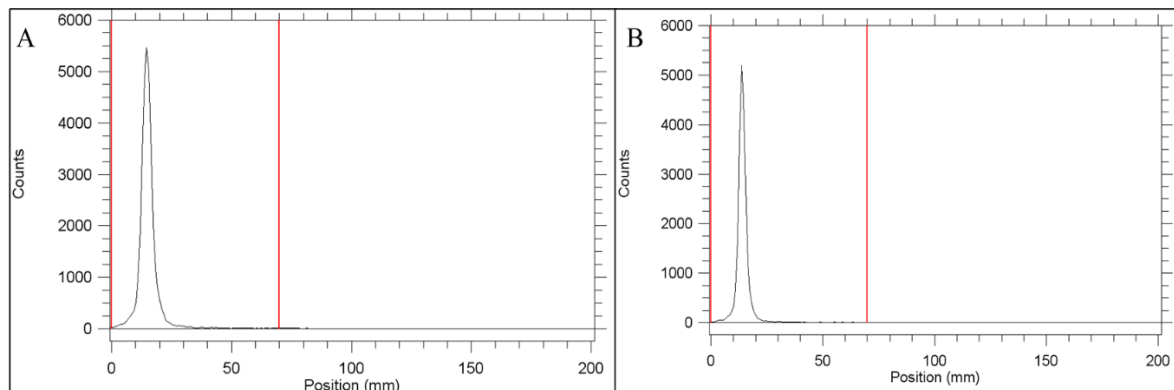


Figure 1. The RTLC chromatogram of A) $[^{99m}\text{Tc}]$ Tc-F1 and B) $[^{99m}\text{Tc}]$ Tc-F2 in the presence of $100 \mu\text{g.mL}^{-1}$ stannous chloride as reducing agent (Stationary phase: ITLC-SG paper - Mobile phase: Acetone)

In one study, $[^{99m}\text{Tc}]$ Tc labeled PLGA nanoparticles were synthesized by Varani *et al.* [29] and labeling efficiency of radiolabeled nanoparticles were evaluated *via* RTLC and found over 97% for 6 h. In another study by Farrak *et al.* [30], $[^{99m}\text{Tc}]$ Tc labeled chitosan nanoparticles were prepared, labeling efficiency were determined using RTLC and found as $93.4 \pm 1.2\%$. According to the literatures, in this study, $[^{99m}\text{Tc}]$ labeled chitosan coated PLGA nanoparticles with high labeling efficiency have been prepared.

2.3. *In vitro* stability studies

Generally, lyophilized kits are dissolved in SF, labeled with $[^{99m}\text{Tc}]$ Tc, and applied to the nuclear medicine patients. Therefore, it is important to know the stability of radiopharmaceuticals in SF. Also, in *in vitro* and *in vivo* studies of radiopharmaceuticals, radiolabeled formulations are incubated with cell medium and serum media during the period of experimentation. The stability of radiolabeled nanoparticles in various media was examined for these reasons, and the results are shown in Figure 2.

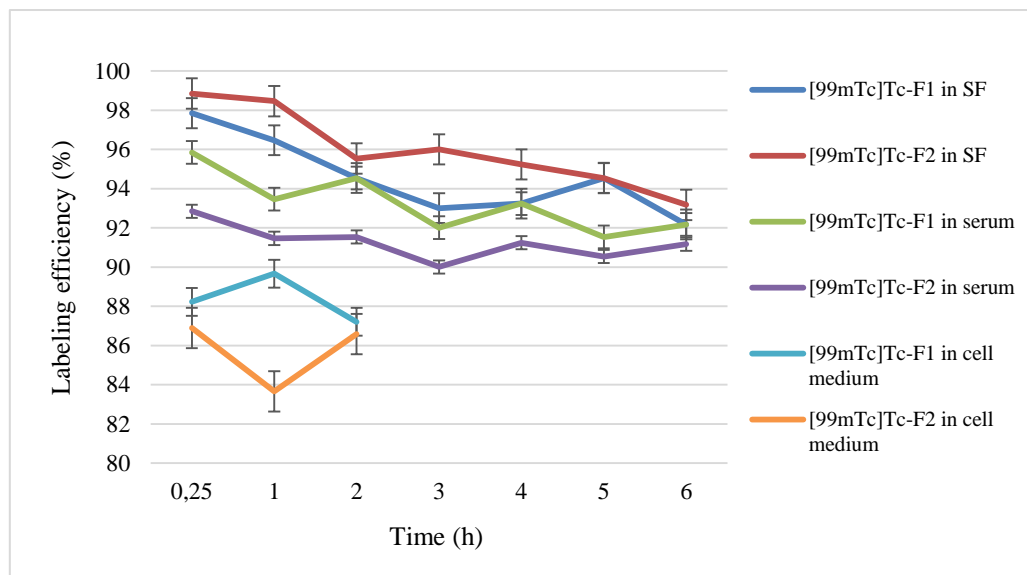


Figure 2. The *in vitro* stability of $[^{99m}\text{Tc}]$ Tc-F1 and $[^{99m}\text{Tc}]$ Tc-F2 in SF, serum, and cell media.

*SF: 0.9% sodium chloride solution, Serum: Fetal bovine serum: phosphate buffer (50:50%, v/v), Cell medium: 10% fetal bovine serum supplemented McCoy's 5A.

As seen in Figure 2, the labeling efficiency of $[^{99m}\text{Tc}]$ Tc-F1 and $[^{99m}\text{Tc}]$ Tc-F2 in SF was revealed between $97.85 \pm 1.89\%$ and $98.85 \pm 1.94\%$ and there was no noticeable change ($p > 0.05$) up to 6 h after radiolabeling. Due to the 6 h stability of both radiolabeled formulations above 90%, they have the feature of being usable even 6 h after preparation in nuclear medicine.

In order to shed light on *in vivo* studies, the *in vitro* stability of $[^{99m}\text{Tc}]$ Tc-F1 and $[^{99m}\text{Tc}]$ Tc-F2 in serum was evaluated and RP of both formulations was found to be higher than 90% up to 6 h (Figure 2).

In addition, radiolabeled formulations are treated with cell media for 2 h in cell culture experiments. The stability of $[^{99m}\text{Tc}]\text{Tc-F1}$ and $[^{99m}\text{Tc}]\text{Tc-F2}$ in cell medium was tested for up to 2 h and found to be quite stable with >80% RP (Figure 2).

2.4. Partition coefficient studies

The $\log P$ value is considered an indicator of the lipophilicity of a compound or formulation and is calculated in drug development studies to shed light on the drug's behavior *in vivo*. A gamma counter was used to detect the $\log P$ of the radiolabeled formulations and R/H- $[^{99m}\text{Tc}]\text{NaTcO}_4$ in this work. The $\log P$ value of $[^{99m}\text{Tc}]\text{Tc-F1}$ and $[^{99m}\text{Tc}]\text{Tc-F2}$ was found -1.499 ± 0.074 and -0.67 ± 0.033 , respectively. As expected, both radiolabeled chitosan coated PLGA based nanoparticle formulations showed very polar characteristics ($\log P < 1$) and results were found to be consistent with previous studies [31]. Also, the $\log P$ value of R/H- $[^{99m}\text{Tc}]\text{NaTcO}_4$ (calculated as a control) was found -2.164 ± 0.108 which also known has hydrophilic properties.

2.5. Cell culture studies

In recent years, *in vitro* cell culture studies have become increasingly relevant in evaluating the cancer binding affinities of radioactive compounds or formulations to shed light on *in vivo* studies [19,31-35]. In this study, the capacity of radiolabeled nanoparticles to bind to MCF-7 cells was investigated. The tests were evaluated for 2 h due to the available half-life of ^{99m}Tc . The cell binding percentage to MCF-7 cell lines of $[^{99m}\text{Tc}]\text{Tc-F1}$, $[^{99m}\text{Tc}]\text{Tc-F2}$ and R/H- $[^{99m}\text{Tc}]\text{NaTcO}_4$ (as a control group) are shown in Figure 3.

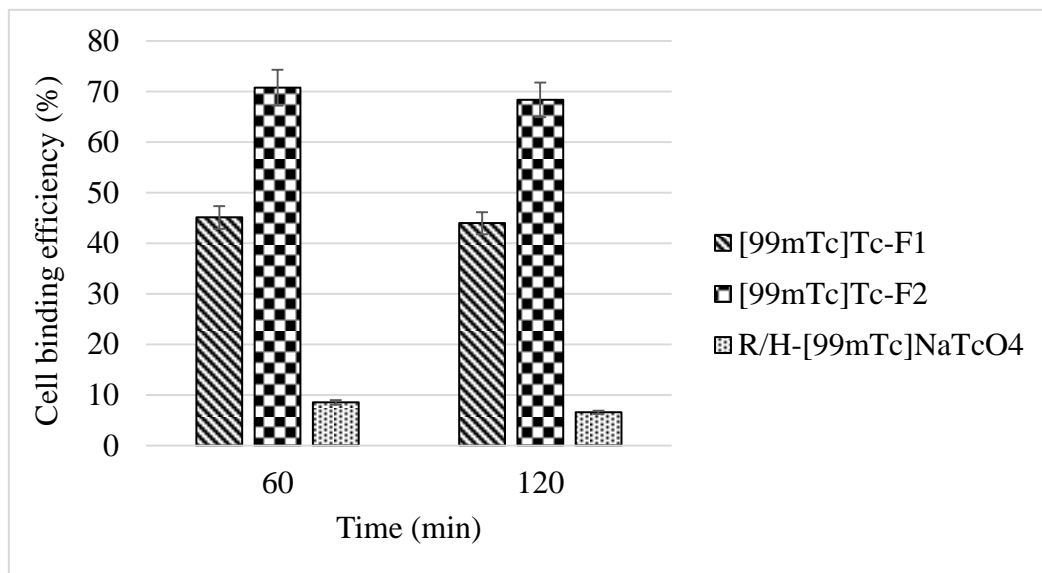


Figure 3. Cell binding capacity of $[^{99m}\text{Tc}]\text{Tc-F1}$, $[^{99m}\text{Tc}]\text{Tc-F2}$ and R/H- $[^{99m}\text{Tc}]\text{NaTcO}_4$ to MCF-7 cell line

As seen in Figure 3, $[^{99m}\text{Tc}]\text{Tc-F2}$ ($70.756 \pm 3.537\%$) have a greater cell binding activity on MCF-7 cells than $[^{99m}\text{Tc}]\text{Tc-F1}$ ($45.091 \pm 2.254\%$) at 60 min. In addition, both nanoparticle formulations retained their percentage of cell binding at 120 min ($[^{99m}\text{Tc}]\text{Tc-F1} = 45.091 \pm 2.197\%$ and $[^{99m}\text{Tc}]\text{Tc-F2} = 68.336 \pm 3.416\%$) due to nanoparticles' passive targeting. Based on these findings, $[^{99m}\text{Tc}]\text{Tc-F1}$ and $[^{99m}\text{Tc}]\text{Tc-F2}$ cannot demonstrate time-dependent variations in cell incorporation and may display substantial accumulation in tumor cells when utilized for tumor imaging. At 60 and 120 min, $[^{99m}\text{Tc}]\text{Tc-F2}$ was found to be more incorporated into breast cancer cell lines than $[^{99m}\text{Tc}]\text{Tc-F1}$. The presence of different molecular weights of PLGA is the only distinction between the two radiolabeled nanoparticles employed in cell culture investigations. So, Figure 3 shows us that chitosan coated PLGA nanoparticles with Resomer® RG 504 H (high molecular weight PLGA) has a higher incorporation activity than chitosan coated PLGA nanoparticles with Resomer® RG 503 H (low molecular weight PLGA) to MCF-7 cells during experimental time. Although they are prepared using polymers of different molecular weights, the characterization and radiolabeling results of F1 and F2 formulations are very close. However, $\log P$ values were different from each other. The $\log P$ value of F1 was found to be -1.499 ± 0.074 while the $\log P$ value of F2 was found to be -0.67 ± 0.033 . These values show us that the F1 formulation is more hydrophilic than the F2 formulation. Thus, F2 formulation has better $\log P$ value than F1 formulation for crossing cytosolic membranes. This difference in cell binding

study can be explained by the less lipophilicity of the F1 formulation and less penetration through the cytoplasmic membrane.

Also, to control the experiment, the percentage of cells incorporated after the application of R/H-[^{99m}Tc]NaTcO₄ was found to be 8.527±0.426% at 60 min and 6.542±0.327% at 120 min. This finding demonstrates that our radiolabeled nanoparticle formulations reacted differently in cell media than R/H-[^{99m}Tc]NaTcO₄ and verified the high labeling efficiency and *in vitro* stability.

3. CONCLUSION

In conclusion, in the presence of 100 µg.mL⁻¹ stannous chloride as a reducing agent, [^{99m}Tc]Tc labeled chitosan coated PLGA nanoparticles were effectively produced, and the labeling efficiency of [^{99m}Tc]Tc-F1 and [^{99m}Tc]Tc-F2 was measured by RTLC and found to be higher than 98%. The radiolabeled formulations were found quite stable in different medium such as SF, serum, and cell medium. The logP value of [^{99m}Tc]Tc-F1 and [^{99m}Tc]Tc-F2 was found -1.499±0.074 and -0.67±0.033, respectively. According to the *in vitro* cell culture studies, [^{99m}Tc]Tc-F2 has greater cell binding activity with a value of ≥70% than [^{99m}Tc]Tc-F1 to MCF-7 cell lines. So, [^{99m}Tc]Tc-F2 may be suggested promising formulations as a cancer imaging agent. However, more study is required such as drug encapsulation and *in vivo* testing.

4. MATERIALS AND METHODS

4.1. Materials

Resomer® RG 503 H [Poly(d,l-lactide-co-glycolide), acid-terminated, lactide:glycolide (PLGA), 50:50, Mw: 24,000–38,000] and Resomer® RG 504 H [PLGA, 50:50, Mw: 38,000] was provided by Sigma-Aldrich (St. Louis, MO, USA). Sigma (Steinheim, Germany) provided low Mw chitosan [Deacetylated chitin/Poly (d-glucosamine), Mw: 50,000–190,000 Da, viscosity: 20–300 cP]. Alfa-Aesar (Kandel, Germany) supplied the Pluronic® F-68. Sigma-Aldrich (Germany) provided the stannous chloride. Adeka (Turkey) provided a 0.9% sodium chloride solution. The [⁹⁹Mo]Mo/[^{99m}Tc]Tc generator at Ege University's Nuclear Medicine Department (Turkey) was used to elute [^{99m}Tc]NaTcO₄. The rest of the compounds were of analytical grade. Gibco Invitrogen (Grand Island, NY) provided cell culture chemicals and supplies. American Type Culture Collection (ATCC) provided the MCF-7 cells.

4.2. Preparation of chitosan coated PLGA nanoparticles

The nanoprecipitation process was used to develop chitosan-coated PLGA-based nanoparticles with some modifications [36–38]. In 3 mL acetone, 90 mg of PLGA was dissolved along with 30 mg of Span® 60. 3 mL of this solution was then put into 10 mL of aqueous phase while being magnetically stirred at 100 rpm, a rate of 1 mL·min⁻¹. 10 mL of 0.25% w/v chitosan solution and 0.5% w/v Pluronic® F-68, both prepared in 2% acetic acid (v/v), were used in the aqueous phase. After that, at room temperature, the acetone was evaporated to dryness for 4 h while being magnetically stirred. The nanoparticles were collected by centrifugation (11,000 rpm, 4°C, 45 min) of the ensuing aqueous dispersion. After collecting the nanoparticles, the particles were washed with distilled water (5 mL). The nanoparticles dispersed in water underwent the same centrifugation procedure as before. To wash the nanoparticles, this process was performed twice. Table 4 lists the substances used in the formulation.

Table 4. Formulation ingredients

Formulations	503 H (mg)	504 H (mg)	Span 60 (mg)	Chitosan (0.25%) (mL)*	ACN (mL)
F1	90	-	30	10	3
F2	-	90	30	10	3

*503 H: Resomer RG 503 H, 504 H: Resomer RG 504 H, Chitosan solution: including Pluronic F-68 (0.5%), ACN: acetone.

4.3. Lyophilization of nanoparticles

Chitosan coated PLGA nanoparticles were resuspended in trehalose solution (3 percent w/v) and were frozen at -80°C. After that, the nanoparticles were lyophilized at -45°C for 48 h at a pressure of 0.07 mbar.

4.4. Characterization of nanoparticles

Dynamic light scattering (DLS) was used to determine the size distribution (PDI), mean size, and zeta potential values of nanoparticle formulations using the Malvern Zetasizer Nano ZS equipment (Malvern Instruments, UK). Using quartz and zeta cuvettes, measurements were made at 25°C with a laser incidence angle of 173°. Before measuring, nanoparticle compositions were diluted in ultrapure water at a 1:400 ratio. The standard deviation (SD) of the mean was calculated. The measurements were carried out five times [39].

4.5. Radiolabeling of nanoparticles

The radiolabeling of nanoparticle formulations was studied to determine the best radiolabeling settings, utilizing the modifications suggested by Ekinci *et al.* [31,32]. In 1 mL 0.9% sodium chloride solution (SF), a sufficient quantity of lyophilized nanoparticles (15 mg) was distributed. Under the influence of a bubbling nitrogen atmosphere, different amounts of stannous chloride solution (10, 25, 50, and 100 µg·mL⁻¹ in pure water) were introduced to the nanoparticle formulations. At neutral pH (pH = 7.0), radiolabeling was conducted with 37 MBq/0.1 [^{99m}Tc]NaTcO₄. The radiolabeled preparation was mixed for 30 seconds before being incubated during 15 min at room temperature. RTLC was used to evaluate the radiolabeling efficiency of nanoparticles at various time intervals (up to 6 h).

4.6. RTLC studies

The stationary phase in the RTLC experiments was ITLC-SG paper. The mobile phase for determining free [^{99m}Tc]NaTcO₄ was acetone while the mobile phase for determining R/H-[^{99m}Tc]NaTcO₄ was pyridine/acetic acid/water (3:5:1.5) solvent mixture. On chromatographic sheets, 2 µL of nanoparticle compositions were spotted using a microcapillary tube, developed in tanks, then air dried. The radioactivity of ITLC-SG chromatographic papers was determined *via* RTLC scanner (Bioscan AR 2000, Washington, DC, USA), and the radiochemical purity (RP) (%) of nanoparticle formulations (^{99m}Tc-F1 and ^{99m}Tc-F2) was calculated using the equation (Equation (1)) [40]:

$$RP (\%) = 100 - (Free [99mTc]NaTcO_4 + reduced/hydrated [99mTc]NaTcO_4) \quad (1)$$

4.7. *In vitro* stability studies

The stability of radiolabeled nanoparticles in diverse settings was tested using cell medium (10% fetal bovine serum (FBS) supplemented McCoy's 5A), SF, and serum medium (FBS: phosphate buffer, (50:50, v/v)). To the mediums (0.4 mL), an amount of 0.1 mL (3.7 MBq) of [^{99m}Tc]Tc-F1 and [^{99m}Tc]Tc-F2 were added. The nanoparticles in the cell medium mixture were incubated at 37°C for 2 h, while the others were incubated at 25°C for 6 h, and RP tests with RTLC were performed throughout the experiment.

4.8. Partition coefficient studies

For the n-octanol/water partition coefficient ($\log P$) investigation, 500 µL each of n-octanol and phosphate buffer (pH 7) were combined in an eppendorf tube, followed by 150 µL of [^{99m}Tc]Tc-F1, [^{99m}Tc]Tc-F2, and R/H-[^{99m}Tc]NaTcO₄ sample. At 25°C, the mixture was shaking for 60 seconds. It was then centrifuged for 30 min at 2.500 rpm. In other tubes, 100 µL of both phases were conveyed. Finally, a gamma counter was used to determine the radioactivity of each phase (Sesa Uniscaller). The measurements were carried out four times. The following Equation (2) was used to compute the $\log P$ of [^{99m}Tc]Tc-F1, [^{99m}Tc]Tc-F2, and R/H-[^{99m}Tc]NaTcO₄ [31]:

$$\log P = \log(radioactivity\ in\ n-octanol\ phase / radioactivity\ in\ buffer\ phase) \quad (2)$$

4.9. Cell culture studies

For cell culture studies, MCF-7 (breast carcinoma) cells were used as a model cancer cell line. The cells in McCoy's 5A were administered a 10% FBS supplement. The cell culture was kept at 37°C with a relative humidity of 90% and a CO₂ concentration of 5%. A 0.25% Trypsin-0.1% EDTA solution was used for subculturing. Seeding 2 × 10⁵ cells on six well plates yielded cell monolayers.

MCF-7 cells were used to conduct cell binding tests using [^{99m}Tc]Tc-F1, [^{99m}Tc]Tc-F2, and R/H-[^{99m}Tc]NaTcO₄ to determine if there was a difference in the incorporation of two different molecular weight

nanoparticles. 7.4 MBq of the radiolabeled samples were incubated with cells at 37°C up to 2 h. After the incubation period, the supernatant was removed from the well plates and placed in a tube. Then, the cells were washed with 1 mL of PBS to separate free [^{99m}Tc]NaTcO₄ and trypsinized with Trypsin-EDTA (0.5 mL) to remove the MCF-7 cells. Also, the cell medium (1 mL) was added, and cells were centrifuged at 3,000 rpm for 5 min. After, the cells were placed in other tube while the supernatant was added the first tube. The amount of radioactivity in tubes was measured *via* gamma counter (Sesa Uniscaller). By dividing the overall activity counted by the fraction of activity counted in the cells, the cellular uptake was calculated. The following equation was used to compute the % radioactivity of cells (Equation (3)) [31,32]:

$$\text{Radioactivity of cells (\%)} = (\text{Radioactivity of cells} / \text{Total radioactivity}) \times 100 \quad (3)$$

4.10. Statistical analysis

Microsoft Excel was used to calculate the means and standard deviations. A one-way ANOVA program was used to establish statistical significance. *p* < 0.05 differences were considered significant. Unless otherwise noted, all experiments were carried out in triplicate.

Acknowledgements: The authors thank to Dr. Hasan Akbaba for cell line (MCF-7) providing and Ege University, Nuclear Medicine Department (Turkey) for radionuclide (^{99m}Tc)NaTcO₄) obtaining.

Author contributions: Concept – M.E., A.A.Ö., D.İ.Ö.; Design – M.E., A.A.Ö., D.İ.Ö.; Supervision – D.İ.Ö.; Resources – M.E., A.A.Ö., D.İ.Ö.; Materials – M.E., A.A.Ö., D.İ.Ö.; Data Collection and/or Processing – M.E., A.A.Ö.; Analysis and/or Interpretation – M.E., A.A.Ö.; Literature Search – M.E.; Writing – M.E., A.A.Ö.; Critical Reviews – M.E., A.A.Ö., D.İ.Ö.

Conflict of interest statement: The authors declared no conflict of interest.

REFERENCES

- [1] Siegel RL, Miller KD, Jemal A. Cancer statistics, 2020. CA Can J Clin. 2020; 70: 7-30. [\[CrossRef\]](#)
- [2] Singh SK, Singh S, Lillard JW Jr, Singh R. Drug delivery approaches for breast cancer. Int J Nanomedicine. 2017; 24: 12: 6205-6218. [\[CrossRef\]](#)
- [3] Lv L, Shi Y, Wu J, Li G. Nanosized drug delivery systems for breast cancer stem cell targeting. Int J Nanomedicine. 2021; 16: 1487-1508. [\[CrossRef\]](#)
- [4] Ekinci M, Santos-Oliveira R, İlem-Özdemir D. Biodistribution of 99mTc-PLA/PVA/Atezolizumab nanoparticles for non-small cell lung cancer diagnosis. Eur J Pharm Biopharm. 2022; 176: 21-31. [\[CrossRef\]](#)
- [5] Ilem-Ozdemir D, Gundogdu EA, Ekinci M, Ozgenc E, Asikoglu M. Nuclear medicine and radiopharmaceuticals for molecular diagnosis. In: Grumezescu AM (ed). Biomedical Applications of Nanoparticles. 1st ed., Elsevier Inc., 2019, pp. 457–490. [\[CrossRef\]](#)
- [6] Jain A, Kunduru KR, Basu A, Mizrahi B, Domb AJ, Khan W. Injectable formulations of poly(lactic acid) and its copolymers in clinical use. Adv Drug Deliv Rev. 2016; 107: 213-227. [\[CrossRef\]](#)
- [7] Akbaba H, Erel-Akbaba G, Kotmakçı M, Başpinar Y. Enhanced cellular uptake and gene silencing activity of survivin-siRNA via ultrasound-mediated nanobubbles in lung cancer cells. Pharm Res. 2020; 37: 165. [\[CrossRef\]](#)
- [8] Ashjari M, Khoei S, Mahdavian AR, Rahmatolahzadeh R. Self-assembled nanomicelles using PLGA-PEG amphiphilic block copolymer for insulin delivery: A physicochemical investigation and determination of CMC values. J Mater Sci Mater Med. 2012; 23: 943-953. [\[CrossRef\]](#)
- [9] Ashjari M, Panahandeh F, Niazi Z, Abolhasani MM. Synthesis of PLGA-mPEG star-like block copolymer to form micelle loaded magnetite as a nanocarrier for hydrophobic anticancer drug. J Drug Deliv Sci Technol. 2020; 56: 101563. [\[CrossRef\]](#)
- [10] Govindarasu M, Abirami P, Alharthi S, Thiruvengadam M, Rajakumar G, Vaiyapuri M. Synthesis, physicochemical characterization, and in vitro evaluation of biodegradable PLGA nanoparticles entrapped to folic acid for targeted delivery of kaempferitrin. Biotechnol Appl Biochem. 2022. [\[CrossRef\]](#)
- [11] Fraguas-Sánchez AI, Torres-Suárez AI, Cohen M, Delie F, Bastida-Ruiz D, Yart L, Martín-Sabroso C, Fernández-Carballedo A. PLGA nanoparticles for the intraperitoneal administration of CBD in the treatment of ovarian cancer: In Vitro and In Vivo assessment. Pharmaceutics. 2020; 12: 439. [\[CrossRef\]](#)

- [12] Şenel B, Öztürk AA. New approaches to tumour therapy with siRNA-decorated and chitosan-modified PLGA nanoparticles. *Drug Dev Ind Pharm.* 2019; 45: 1835-1848. [\[CrossRef\]](#)
- [13] Moshiri M, Mehmammadnavaz F, Hashemi M, Yazdian-Robati R, Shabazi N, Etemad L. Evaluation of the efficiency of simvastatin loaded PLGA nanoparticles against acute paraquat-intoxicated rats. *Eur J Pharm Sci.* 2022; **168**: 106053. [\[CrossRef\]](#)
- [14] Sharifianjazi F, Khaksar S, Esmaeilkhanian A, Bazli L, Eskandarinezhad S, Salahshour P, Sadeghi F, Rostamnia S, Vahdat SM. Advancements in fabrication and application of chitosan composites in implants and dentistry: A review. *Biomolecules.* 2022; **12**: 155. [\[CrossRef\]](#)
- [15] Yee Kuen C, Masarudin MJ. Chitosan nanoparticle-based system: A new insight into the promising controlled release system for lung cancer treatment. *Molecules.* 2022; **27**: 473. [\[CrossRef\]](#)
- [16] Yang F, Cabe M, Nowak HA, Langert KA. Chitosan/poly(lactic-co-glycolic)acid nanoparticle formulations with finely-tuned size distributions for enhanced mucoadhesion. *Pharmaceutics.* 2022; **14**: 95. [\[CrossRef\]](#)
- [17] Zare S, Kabiri M, Amini Y, Najafi A, Mohammadpour F, Ayati SH, Nikpoor AR, Tafaghodi M. Immunological assessment of chitosan or trimethyl chitosan-coated plga nanospheres containing fusion antigen as the novel vaccine candidates against tuberculosis. *AAPS PharmSciTech.* 2021; **23**: 15. [\[CrossRef\]](#)
- [18] Elitez Y, Ekinci M, İlem-Ozdemir D, Gundogdu E, Asikoglu M. Tc-99m radiolabeled alendronate sodium microemulsion: Characterization and permeability studies across caco-2 cells. *Curr Drug Deliv.* 2018; **15**: 342-350. [\[CrossRef\]](#)
- [19] İlem-Özdemir D, Karavana SY, Şenyigit ZA, Çalışkan Ç, Ekinci M, Asikoglu M, Baloglu E. Radiolabeling and cell incorporation studies of gemcitabine HCl microspheres on bladder cancer and papilloma cell line. *J Radioanal Nucl Chem.* 2016; **310**: 515-522. [\[CrossRef\]](#)
- [20] Alshamsan A. Nanoprecipitation is more efficient than emulsion solvent evaporation method to encapsulate cucurbitacin I in PLGA nanoparticles. *Saudi Pharm J.* 2014; **22**: 219-222. [\[CrossRef\]](#)
- [21] Bilati U, Allémann E, Doelker E. Development of a nanoprecipitation method intended for the entrapment of hydrophilic drugs into nanoparticles. *Eur J Pharm Sci.* 2005; **24**: 67-75. [\[CrossRef\]](#)
- [22] Luque-Alcaraz AG, Lizardi-Mendoza J, Goycoolea FM, Higuera-Ciapara I, Argüelles-Monal W. Preparation of chitosan nanoparticles by nanoprecipitation and their ability as a drug nanocarrier. *RSC Adv.* 2016; **6**: 59250-59256. [\[CrossRef\]](#)
- [23] Martínez Rivas CJ, Tarhini M, Badri W, Miladi K, Greige-Gerges H, Nazari QA, Galindo Rodríguez SA, Román RA, Fessi H, Elaissari A. Nanoprecipitation process: From encapsulation to drug delivery. *Int J Pharm.* 2017; **532**: 66-81. [\[CrossRef\]](#)
- [24] Miladi K, Sfar S, Fessi H, Elaissari A. Nanoprecipitation process: from particle preparation to in vivo applications. In: Vauthier C, Ponchel G (eds). *Polymer Nanoparticles for Nanomedicines*, Springer International Publishing, 2016, pp. 17-53.
- [25] Mora-Huertas CE, Fessi H, Elaissari A. Polymer-based nanocapsules for drug delivery. *Int J Pharm.* 2010; **385**: 113-142. [\[CrossRef\]](#)
- [26] Martín-Banderas L, Álvarez-Fuentes J, Durán-Lobato M, Prados J, Melguizo C, Fernández-Arévalo M, Holgado MÁ. Cannabinoid derivate-loaded PLGA nanocarriers for oral administration: formulation, characterization, and cytotoxicity studies. *Int J Nanomed.* 2012; **7**: 5793-5806. [\[CrossRef\]](#)
- [27] Bhattacharjee S. DLS and zeta potential? What they are and what they are not?. *J Controlled Release.* 2016; **235**: 337-351. [\[CrossRef\]](#)
- [28] Zolle U. *Technetium-99m pharmaceuticals: Preparation and quality control in nuclear medicine*. Springer, Berlin, Heidelberg, 2007. [\[CrossRef\]](#)
- [29] Varani M, Campagna G, Bentivoglio V, Serafinelli M, Martini ML, Galli F, Signore A. Synthesis and biodistribution of 99mTc-labeled PLGA nanoparticles by microfluidic technique. *Pharmaceutics.* 2021; **13**: 1769. [\[CrossRef\]](#)
- [30] Farrag NS, Shetta A, Mamdouh W. Green tea essential oil encapsulated chitosan nanoparticles-based radiopharmaceutical as a new trend for solid tumor theranosis. *Int J Biol Macromol.* 2021; **186**: 811-819. [\[CrossRef\]](#)
- [31] Ekinci M, Öztürk AA, Santos-Oliveira R, İlem-Özdemir D. The use of Lamivudine-loaded PLGA nanoparticles in the diagnosis of lung cancer: Preparation, characterization, radiolabeling with 99mTc and cell binding. *J Drug Deliv Sci Technol.* 2022; **69**: 103139. [\[CrossRef\]](#)

- [32] Ekinci M, Ilem-Ozdemir D, Gundogdu E, Asikoglu M. Methotrexate loaded chitosan nanoparticles: Preparation, radiolabeling and in vitro evaluation for breast cancer diagnosis. *J Drug Deliv Sci Technol.* 2015; 30: 107-113. [\[CrossRef\]](#)
- [33] Ari K, Ucar E, Ichedef C, Kilcar AY, Medine EI, Parlak Y, Bilgin BES, Aydin B, Gumuser FG, Teksoz S. Tc-99m(I) carbonyl-radiolabeled lipid based drug carriers for temozolomide delivery and bioevaluation by in vitro and in vivo. *Radiochimica Acta.* 2019; 107: 1185-1193. [\[CrossRef\]](#)
- [34] Jackson MR, Bavelaar BM, Waghorn PA, Gill MR, El-Sagheer AH, Brown T, Tarsounas M, Vallis KA. Radiolabeled oligonucleotides targeting the RNA subunit of telomerase inhibit telomerase and induce DNA damage in telomerase-positive cancer cells. *Cancer Res.* 2019; 79: 4627-4637. [\[CrossRef\]](#)
- [35] Bansal A, Pandey MK, Demirhan YE, Nesbitt JJ, Crespo-Diaz RJ, Terzic A, Behfar A, DeGrado TR. Novel 89Zr cell labeling approach for PET-based cell trafficking studies. *EJNMMI Res.* 2015; 5: 19. [\[CrossRef\]](#)
- [36] de Lima IA, Khalil NM, Tominaga TT, Lechanteur A, Sarmento B, Mainardes RM. Mucoadhesive chitosan-coated PLGA nanoparticles for oral delivery of ferulic acid. *Artif Cells Nanomedicine Biotechnol.* 2018; 46: 993-1002. [\[CrossRef\]](#)
- [37] Durán-Lobato M, Martín-Banderas L, Gonçalves LMD, Fernández-Arévalo M, Almeida AJ. Comparative study of chitosan-and PEG-coated lipid and PLGA nanoparticles as oral delivery systems for cannabinoids. *J Nanoparticle Res.* 2015; 17: 1-17. [\[CrossRef\]](#)
- [38] Khan N, Ameeduzzafar, Khanna K, Bhatnagar A, Ahmad FJ, Ali A. Chitosan coated PLGA nanoparticles amplify the ocular hypotensive effect of forskolin: Statistical design, characterization and in vivo studies. *Int J Biol Macromol.* 2018; 116: 648-663. [\[CrossRef\]](#)
- [39] Carvalho PM, Felício MR, Santos NC, Gonçalves S, Domingues MM. Application of light scattering techniques to nanoparticle characterization and development. *Front Chem.* 2018; 6: 237. [\[CrossRef\]](#)
- [40] Kakkar V, Mishra AK, Chuttani K, Kaur IP. Proof of concept studies to confirm the delivery of curcumin loaded solid lipid nanoparticles (C-SLNs) to brain. *Int J Pharm.* 2013; 448: 354-359. [\[CrossRef\]](#)

This is an open access article which is publicly available on our journal's website under Institutional Repository at <http://dspace.marmara.edu.tr>.